

Optimum excitation conditions for the generation of high-electric-field terahertz radiation from an oscillator-driven photoconductive device

André Dreyhaupt, Stephan Winnerl, and Manfred Helm

Institute of Ion Beam Physics and Materials Research, Forschungszentrum Rossendorf, P.O. Box 510119, 01314 Dresden, Germany

Thomas Dekorsy

Universität Konstanz, Fachbereich Physik, 78457 Konstanz, Germany

Received January 3, 2006; accepted February 15, 2006; posted March 1, 2006 (Doc. ID 66900)

We report the impulsive generation of terahertz (THz) radiation with a field amplitude of more than 1.5 kV/cm at megahertz repetition rates, using an interdigitated photoconducting device. The approach provides an average THz power of 190 μ W, corresponding to an optical-to-THz conversion efficiency of 2.5×10^{-4} . Optimum conditions are achieved when the excitation spot size is of the order of the THz wavelength. © 2006 Optical Society of America

OCIS codes: 300.6270, 260.5150, 320.7130.

Impulsive terahertz (THz) sources have undergone significant improvements over the past decade. For example, field amplitudes up to 400 kV/cm have been demonstrated by four-wave mixing in ionized air by using amplified laser systems.¹ For many applications oscillator-based THz systems are preferable, since they are less complex and allow high signal-to-noise ratios to be achieved. To this end, several new approaches to photoconductor (PC)-based THz emitters excited by high-repetition-rate femtosecond oscillators have been presented.^{2,3} THz applications range from novel materials⁴ and spectroscopy⁵ to imaging.⁶ In this Letter we report a PC THz emitter operated at moderate voltages and a megahertz repetition rate, providing high THz electric fields and power.

Our concept is based on an interdigitated gold finger electrode structure with 150 nm thickness and 5 μ m electrode spacing fabricated on a semi-insulating GaAs substrate followed by a Si₃N₄ insulation layer of 1 μ m thickness. A further metallization covers every second finger electrode spacing. The active area of this structure is 3 mm \times 3 mm, and it provides a THz source that is operated by a femtosecond near-infrared (NIR) laser system (800 nm central wavelength, 65 fs full width at half-maximum (FWHM) pulse duration, 78 MHz repetition rate, maximum 800 mW average power). Hence a broadband single-cycle electromagnetic wave is emitted by the photoexcited carriers, accelerated in the electric field between the electrodes. Owing to the opaque second gold metallization on top of the finger electrodes, photoexcitation takes place only in uniform field regions. The resulting THz radiation interferes constructively in the far field. This device overcomes disadvantages inherent to emitters using photoconductive antennas (usually low power) and large-aperture emitters using two stripe electrodes (limited bandwidth, high voltages required). A detailed de-

scription of the emitter concept was given in an earlier paper.⁷

Two off-axis parabolic mirrors (50 and 25 mm effective focal length) are used to focus the THz radiation to the detection system as shown in the inset of Fig. 1(a). A small fraction of the laser beam is split off for the THz detection. This optical beam is realigned with the THz beam by a tin-doped indium oxide (ITO) coated mirror.⁸ The THz detection is performed by conventional electro-optic sampling^{9,10} (EOS), using a 25 μ m ZnTe (110) crystal on fused silica, a polarizing beam splitter, two balanced photodiodes, and a lock-in amplifier locked to the 10 kHz modulation of the THz emitter bias. The duty cycle of the bias was 10% to limit the power dissipation that may reduce the THz output. The setup was purged with nitrogen to reduce the absorption of THz radiation by atmospheric water vapor.

Figure 1(a) shows the THz electric field at different acceleration fields. For a bias of 30 V (60 kV/cm) and $4 \times 10^{17}/\text{cm}^3$ excitation density within a 300 μ m (FWHM) NIR spot, a THz electric field of 1.7 kV/cm was deduced by using the method described in Ref. 2. Until now this is the largest THz field reported in the literature (to our knowledge) for an oscillator-excited THz source operated at megahertz repetition rates. The strong increase of the detected THz field compared with that of our earlier paper⁷ (85 V/cm at 100 mW excitation power) is based on the optimization of the excitation conditions (see discussion below). However, a maximum signal-to-noise ratio is achieved by using a thicker ZnTe analyzer and a 50% duty cycle. That is to say, with a 1 mm ZnTe crystal and 50% duty cycle the signal-to-noise ratio is about 3×10^4 , measured within 25 s. The measurement time is limited by the slow optical delay in step-scan mode. This corresponds to a 2% differential signal at the photodiodes. The resulting spectra in Fig. 1(b) show broadband frequency characteristics with a

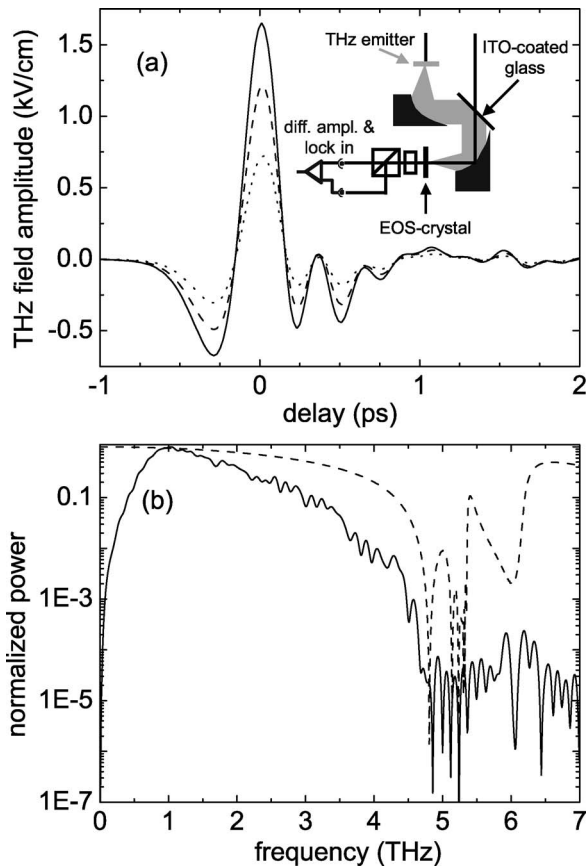


Fig. 1. (a) Time-domain THz waveform for acceleration fields of 20 kV/cm (dotted), 40 kV/cm (dashed), and 60 kV/cm (solid) at an excitation density of $4 \times 10^{17} \text{ cm}^{-3}$. (b) Power spectra calculated from the time-domain data of (a) for 60 kV/cm. The dashed curve represents the calculated response of the ZnTe analyzer crystal.

10 dB bandwidth of 2.5 THz. Apart from that the spectra are influenced by phonons of the ZnTe crystal, the mismatch of the phase and group velocity of the THz and NIR beams, respectively and residual water vapor in the setup.

The calculation of the response of the ZnTe EOS crystal takes into account the velocity mismatch of the THz wave and the 800 nm radiation and the frequency dependence of the electro-optic coefficient r_{41} and of the reflections of the THz beam.¹⁰ The pulse duration of the probe beam (65 fs) is included. Material constants in the calculation are taken from Ref. 10 and references therein, except for the high-frequency dielectric constant of ZnTe, where $\epsilon_{\infty} = 7.3$ is used¹¹ to fit our experimental data. The group velocity dispersion of ZnTe in the wavelength region around 800 nm is modeled by a quadratic fit to experimental data for the refractive index of Ref. 11. These data are in good agreement with more recent experimental studies.^{12,13} We tested our model by comparing the calculated response with experimental spectra for different ZnTe thicknesses (not shown) and found very good agreement. As indicated in Fig. 1(b), the emitted THz radiation extends up to 4.5 THz.

The spatial distribution of the THz spot at the electro-optic sensor was mapped by steering the THz

beam with the ITO mirror while keeping the NIR probe beam unchanged. The THz beam has an elliptical Gaussian shape as displayed in the inset of Fig. 2, with sizes of 340 and 410 μm FWHM. From the knowledge of the temporal evolution, spatial distribution, and maximum electric field of the THz pulse, we have calculated the average THz power within the bias pulse to 190 μW for an optical excitation power of 775 mW and an acceleration field of 60 kV/cm. This corresponds to a NIR-to-THz power-conversion efficiency of about 2.5×10^{-4} . It should be noted that in the present device less than 20% of the incident radiation is absorbed in the PC due to 75% coverage of the surface with metallization and the reflectivity of the PC. This value can be enhanced by using an asymmetric finger structure minimizing the shadowed region between the electrodes and by adapting the dielectric cover layers to an antireflection coating. Only recently a power-conversion efficiency of about 7×10^{-4} was published by Kim *et al.*³ for line-shape excitation near one electrode of a coplanar antenna. However, the emitted THz power was only of the order of 10 μW .

We have also measured the emitted THz power directly by using a pyroelectric detector (Fig. 2) and found a quadratic dependence on the optical excitation power. For an excitation power of 800 mW and an acceleration field of 40 kV/cm we have achieved an average THz power of 24 μW . Taking into account the different parameters (electric field and duty cycle), the power measured with the pyroelectric detector was about 3.5 times smaller than the value obtained from the EOS measurement, which is probably due to an insufficient free aperture of the detector and an uncertainty in the calibration.

To find the optimal operating conditions, we have investigated the dependence of the THz field on the radius a of the optically excited area. The THz emission of our source can be treated as transmission through a hole in the limiting cases $a \ll \lambda$ and $a \gg \lambda$. For $a \gg \lambda$ all radiated frequency components can propagate to the far field. Assuming a circular excitation spot and an invariant THz beam profile at the

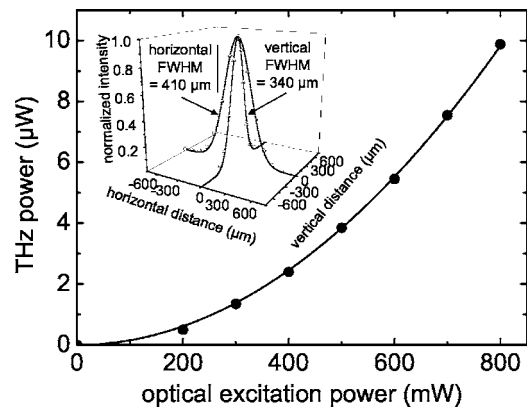


Fig. 2. Dependence of the THz power (measured with a pyroelectric detector) on excitation power using an acceleration field of 20 kV/cm. Filled circles, measured data; solid curve, second-order polynomial. Inset, beam profile of the THz spot at the electro-optic sensor.

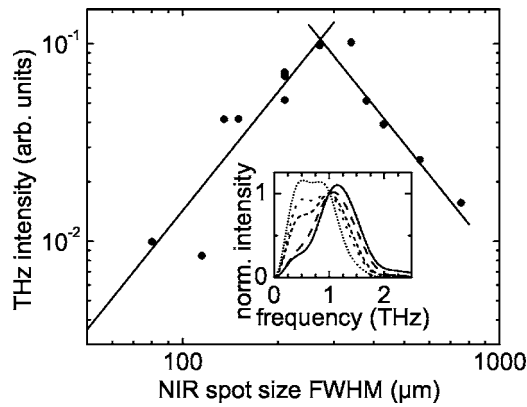


Fig. 3. Dependence of the detected THz intensity (E_{THz}^2) on the size (FWHM) of the exciting NIR spot (double logarithmic scale). Filled circles, measured data; solid lines, guides to the eyes. Inset, THz spectra for various excitation spot sizes normalized to the intensity value at 1 THz; 755 μm (short dotted), 560 μm (dotted), 430 μm (short dashed), 210 μm (dashed), 115 μm (solid).

electro-optic crystal, the NIR power P_{NIR} is related to the THz intensity I_{THz} by

$$P_{\text{NIR}}/\pi a^2 = I_{\text{NIR}},$$

$$I_{\text{NIR}} \propto n \propto E_{\text{THz}}, \quad E_{\text{THz}}^2 \propto I_{\text{THz}}, \quad (1)$$

where I_{NIR} is the optical intensity, n is the carrier density, and E_{THz} is the THz electric field. Assuming that the THz radiating area equals half the optically excited area, the THz power P_{THz} is given by

$$P_{\text{THz}} = \frac{\pi a^2}{2} I_{\text{THz}},$$

and with Eq. (1),

$$P_{\text{THz}} \propto P_{\text{NIR}}^2/a^2. \quad (2)$$

Thus for a given optical power the THz power decreases with $1/a^2$. If $a \ll \lambda$ the wave propagation is diffraction limited. This is reflected in the spectra shown in the inset of Fig. 3, which exhibit a blueshift for smaller excitation spots, because only short wavelengths propagate to the far field. The THz power in the far field is proportional to a^2 , since an additional factor as derived by Bethe¹⁴ and recently discussed by García de Abajo¹⁵ with an a^4 dependence enters Eq. (2).

Therefore the maximum power-conversion efficiency is achieved for an excitation spot size of the order of the central THz wavelength ($\approx 300 \mu\text{m}$ in our experiments) as long as the emitter is not saturated owing to screening. However, amplifier-driven systems may use larger excitation spot sizes to prevent saturation¹⁶ and achieve higher output with a similar conversion efficiency if I_{NIR} is kept constant. We have measured the THz intensity for different optical spot sizes in between the above limiting cases; thus the above discussion does not strictly apply. However, Fig. 3 exhibits a maximum at about 300 μm and a de-

crease of the THz intensity for smaller and larger spot sizes. A similar behavior was reported for optical rectification experiments by Xu and Zhang.¹⁷ In contrast to our investigations they measured the THz power (as opposed to the intensity).

Large-aperture THz emitters typically exhibit THz spectra¹⁶ centered at relatively low frequencies. This is usually attributed to the low acceleration field within the large distance between the electrodes. However, those emitters are usually excited by a large NIR spot, which as well enhances the fraction emitted at low frequencies (<1 THz). On the other hand, the excellent properties of the semilarge-aperture GaAs emitter proposed by Planken *et al.*² can be ascribed to the fact that the excitation spot size is of the order of the main THz emission wavelength.

In summary we have presented a bright source of THz radiation with a kilovolt per centimeter THz field amplitude and high power efficiency excited by an oscillator at a megahertz repetition rate. It has been demonstrated that the optimum excitation spot size is of the order of the central wavelength of the THz wave.

We acknowledge valuable discussion with C. Kübler and R. Huber concerning the preparation of thin ZnTe crystals. S. Winner's e-mail address is s.winnerl@fz-rossendorf.de; A. Dreyhaupt's e-mail address is a.dreyhaupt@fz-rossendorf.de.

References

1. T. Bartel, P. Gaal, K. Reimann, M. Woerner, and T. Elsaesser, *Opt. Lett.* **30**, 2805 (2005).
2. P. C. M. Planken, C. E. W. M. van Rijmenam, and R. N. Schouten, *Semicond. Sci. Technol.* **20**, S121 (2005), and references therein.
3. J. H. Kim, A. Polley, and S. E. Ralph, *Opt. Lett.* **30**, 2490 (2005).
4. H. O. Moser, B. D. F. Casse, O. Wilhelmi, and B. T. Saw, *Phys. Rev. Lett.* **94**, 063901 (2005).
5. N. Sekine and K. Hirakawa, *Phys. Rev. Lett.* **94**, 057408 (2005).
6. M. Usami, M. Yamashita, K. Fukushima, C. Otani, and K. Kawase, *Opt. Lett.* **86**, 141109 (2005).
7. A. Dreyhaupt, S. Winnerl, T. Dekorsy, and M. Helm, *Appl. Phys. Lett.* **86**, 121114 (2005).
8. T. Bauer, J. S. Kolb, T. Löffler, E. Mohler, H. G. Roskos, and U. C. Pernisz, *J. Appl. Phys.* **92**, 2210 (2002).
9. Q. Wu and X.-C. Zhang, *Appl. Phys. Lett.* **68**, 1604 (1996).
10. A. Leitenstorfer, S. Hunsche, J. Shah, M. C. Nuss, and W. H. Knox, *Appl. Phys. Lett.* **74**, 1516 (1999).
11. T. R. Sliker and J. M. Jost, *J. Opt. Soc. Am.* **56**, 130 (1966).
12. K. Sato and S. Adachi, *J. Appl. Phys.* **73**, 926 (1993).
13. Q. Wu and X.-C. Zhang, *IEEE J. Solid-State Circuits* **2**, 693 (1996).
14. H. A. Bethe, *Phys. Rev.* **66**, 163 (1944).
15. F. J. García de Abajo, *Opt. Express* **10**, 1475 (2002).
16. T. Löffler, M. Kreß, M. Thomson, T. Hahn, N. Hasegawa, and H. G. Roskos, *Semicond. Sci. Technol.* **20**, S134 (2005).
17. J. Z. Xu and X.-C. Zhang, *Opt. Lett.* **27**, 1067 (2002).